Critical energies in elastic α-nucleus scattering

Takigawa, N; Put, LW

Published in:
Physics Letters B

DOI:
10.1016/0370-2693(79)91218-8

Publication date:
1979

CRITICAL ENERGIES IN ELASTIC α–NUCLEUS SCATTERING

N. TAKIGAWA
Universität Münster, Institut für Theoretische Physik I, 4400 Münster, West-Germany and Tohoku University, Department of Physics, 980 Sendai, Japan

and

L.W. PUT
Kernfysisch Versneller Instituut, Rijksuniversiteit Groningen, Groningen, The Netherlands

Received 21 March 1979
Revised manuscript received 9 May 1979

The semiclassical theory is used to introduce two critical energies elucidating the energy dependence of the angular distribution and of the scattering mechanism for elastic scattering of α-particles from nuclei. Experimental data are confronted with this concept.

The angular distribution of the elastic scattering of α-particles from nuclei shows a typical variation with the bombarding energy [1], which is common to many target nuclei. As already discussed by Goldberg et al. [2,3], an interesting quantity in understanding the energy variation of the angular distribution is the energy whose corresponding grazing angular momentum is the lowest partial wave which has no potential pocket in the energy surface. Let us call this the first critical energy $\epsilon_{\mathrm{crit}}^{(1)}$. For the optical potential which fits α–^{90}Zr scattering data $\epsilon_{\mathrm{crit}}^{(1)}$ is around 80 MeV. The structure of the angular distribution in fact drastically changes as the incident energy crosses this energy (see fig. 1 of ref. [1]).

The fairly complicated angular distribution over the whole angular range observed at energies lower than $\epsilon_{\mathrm{crit}}^{(1)}$ has been interpreted in terms of the interference between the waves reflected at the external potential barrier (the barrier waves) and the waves reflected by the internal centrifugal potential barrier (the internal waves) [4,5]. In the semiclassical analysis of the relevant data there exist three important turning points for each partial wave, especially for surface partial waves (see fig. 1). For energies above $\epsilon_{\mathrm{crit}}^{(1)}$ the differential cross section strongly oscillates at forward angles, shows a gross hump at medium angles, and then monotonically decreases with angle. This pattern has been observed for energies up to 166 MeV [1,3,6], the highest energy for which experimental data are available at this moment. The gross hump has been attributed to a nuclear rainbow effect [2,3,7]. We have calculated the differential cross section for α-scattering from ^{90}Zr for energies between 170 MeV and 300 MeV by using optical potentials with an average Woods–Saxon form factor given by [1]

$$r_{\mathrm{R}} = 1.245 \text{ fm}, \quad a_{\mathrm{R}} = 0.801 \text{ fm},$$

$$r_{\mathrm{w}} = 1.570 \text{ fm}, \quad a_{\mathrm{w}} = 0.567 \text{ fm}. \tag{1a}$$

The values of the strength of the real and imaginary potentials V_0 and W_0 were taken as

$$V_0(E_\alpha) = 155.2(1 - 0.0016\, E_\alpha)\,, \tag{1b}$$

$$W_0(E_\alpha) = 19.2(1 + 0.0003\, E_\alpha)\,, \tag{1c}$$

which well represent the V_0 and W_0 values at 80–142 MeV [1]. The feature of the angular distributions thus obtained for these high energies is essentially the same as that for energies between $\epsilon_{\mathrm{crit}}^{(1)}$ and 166 MeV.

In this letter, we will be mainly concerned with the

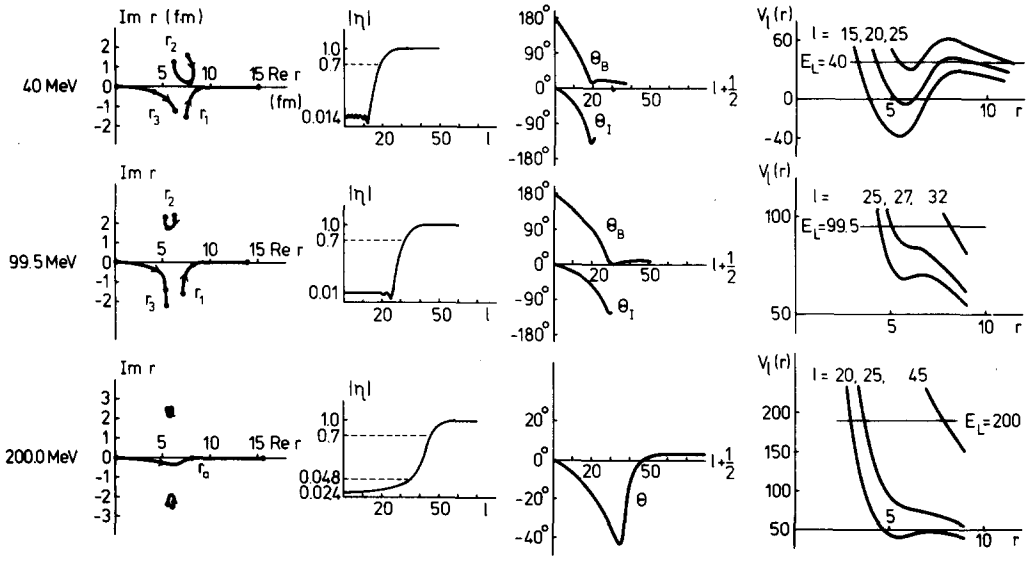

Fig. 1. Comparison of the distribution of turning points, the absolute value of the total S matrix $|\eta|$ as a function of the angular momentum, the classical deflection functions and energy surfaces for a few partial waves at three typical energies for $\alpha + {}^{90}Zr$ scattering.

scattering mechanism above the first critical energy. We will show that the incident energy has to be much higher than $\epsilon^{(1)}_{crit}$ in order that one could interpret the gross hump at medium angles in terms of a nuclear rainbow effect. In this connection, we introduce a second critical energy $\epsilon^{(2)}_{crit}$, the basic idea of which is as follows. When the incident energy is not so far above $\epsilon^{(1)}_{crit}$, the existence of the external potential barrier should still be felt and a fraction of the incident waves should be reflected there. In the language of semiclassical theory, for some partial waves there are still three important turning points and the interference between the barrier and the internal waves still plays an important role. At very high energy, the existence of the external potential barrier should, of course, not be felt at all and there is only one turning point for each partial wave. We define the second critical energy, $\epsilon^{(2)}_{crit}$, as the energy where one turning point becomes sufficient. In what follows we use the nomenclature energy region I, II and III to denote energies below $\epsilon^{(1)}_{crit}$, between $\epsilon^{(1)}_{crit}$ and $\epsilon^{(2)}_{crit}$ and above $\epsilon^{(2)}_{crit}$, respectively.

The calculations reported in this letter were made for $\alpha + {}^{90}Zr$ scattering, but the general idea is applicable to other systems as well. Fig. 1 shows the trajectories of the turning points, the absolute value of the total S matrix η as a function of the angular momentum l, the classical deflection function θ, and effective potential surfaces for three typical incident energies [‡1]. On each trajectory of turning points, there exists one turning point for each partial wave. The arrows on the trajectories of turning points indicate the direction of movement of the turning point with increasing angular mometum. The thick dot at the middle of the trajectories is the turning point for the partial wave for which $|\eta|$ is $2^{-1/2}$. For $E_\alpha = 200$ MeV there exists a trajectory r_a in the vicinity of the real axis. The other trajectories of turning points are so far away from the real axis that one can disregard them. The S matrix is thus simply given by

$$\eta(l) = \eta_a(l) = e^{2i\sigma(l)} e^{2i\delta_a(l)}, \qquad (2)$$

where $\sigma(l)$ is the Coulomb phase shift and the nuclear phase shift $\delta_a(l)$ is given by the conventional JWKB formula with respect to the complex turning point r_a.

At 99.5 MeV, though the angular distribution looks quite similar to that at 200 MeV, one needs to take into account three turning points. In this respect the

[‡1] The optical potential parameters given by eq. (1) have been used for these calculations, except for $E_\alpha = 40$ MeV for which the best-fit parameters of ref. [1] were used.

situation is similar to that at 40 MeV. The total S matrix is therefore given as a sum of two terms [4,5],

$$\eta(l) = \eta_B(l) + \eta_I(l) , \quad (3)$$

where the barrier and the internal wave S matrices η_B and η_I are given by

$$\eta_B(l) = e^{2i\sigma(l)}\, e^{2i\delta_1(l)}/N = \eta_B^{(0)}(l)/N , \quad (4)$$

$$\eta_I(l) = e^{2i\sigma(l)}\, (e^{2i\delta_1(l)}/N)\, e^{2iS_{21}}\, (e^{2iS_{32}}/N) . \quad (5)$$

In eqs. (4) and (5) δ_1 is the conventional JWKB phase shift with respect to r_1. S_{ij} is the classical action integral between the complex turning points r_i and r_j. The barrier penetration factor N is given as a function of $z = S_{21}/\pi$ [4]. Though it is not so decisive as in the energy region I, it is still not negligible for intermediate partial waves. The r.h.s. of eq. (5) should in general be multiplied by the enhancement factor h, which represents the effect of multiple reflection of waves inside the potential well. This factor is almost unity in our present example, so that we have not explicitly written it in eq. (5).

The oscillations in the absolute value of the total S matrix have been attributed to the interference between the barrier and the internal wave S matrices [4,5,8]. The oscillations observed in $|\eta|$ for $E = 99.5$ MeV thus clearly indicate that the splitting of the total S matrix into a sum of the barrier and the internal wave S matrices is still meaningful at this energy and the interference of these waves is expected to play an important role in producing the final angular distribution (see fig. 2). Differently from the case of low energies, e.g. at 40 MeV, oscillations appear only for surface partial waves in $|\eta|$ for 99.5 MeV. This is because $|\eta_B|$ at this energy is very small for low partial waves.

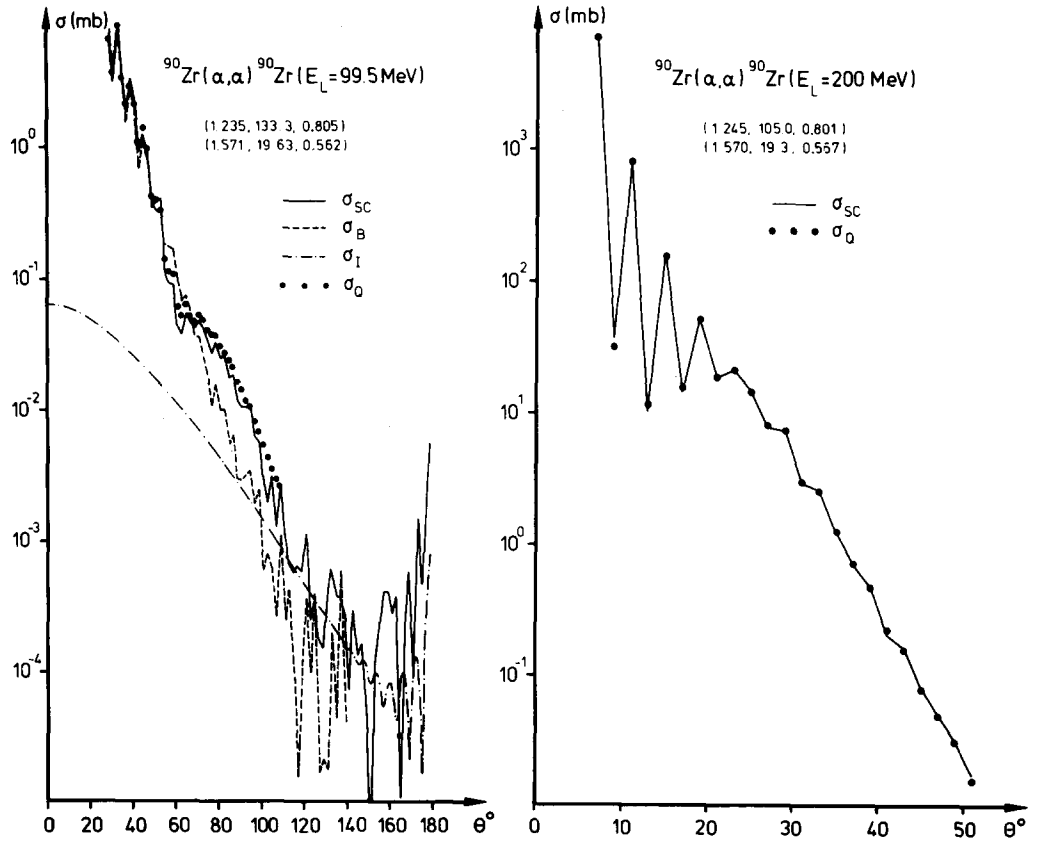

Fig. 2. Decomposition of the differential cross section and comparison between semiclassical and quantum calculations.

At 200 MeV $|\eta|$ is a monotonic function of the angular momentum l. This is a natural consequence of the fact that there exists only one important turning point for each l at this energy. The oscillation amplitude is about 10, 3 and 1% at 155, 160 and 165 MeV, respectively. The oscillation disappears above 170 MeV. The second critical energy for α–^{90}Zr scattering is thus around 165 MeV.

Though the existence of the external potential barrier leads to a distribution of turning points for medium energies similar to that for low energies, the role of the external potential barrier is clearly less important in energy region II. The consequence is, for example, that the behaviour of $|\eta_B(l)|$ in region II as a function of l is mainly determined by the imaginary potential. In this sense, the S matrix $\eta_B(l)$ at medium energies describes a reflective–diffractive scattering and might correspond to the diffractive S matrix $S_D(\lambda)$ discussed in ref. [9]. Similarly, the function $|\eta_a(l)|$ in region III is also mainly governed by the imaginary potential. This can be seen more explicitly as follows. We first notice that the behaviour of $|\eta_a(l)|$ and $|\eta_B(l)|$ in region III and II, respectively, looks similar to that of the smooth cut-off model for the S matrix [10]. In energy region II $|N|$ is nearly one for all partial waves, so that the behaviour of $|\eta_B(l)|$ as a function of l is almost the same as that of $|\eta_B^{(0)}(l)|$. We then define the cut-off angular momentum L_c and the diffuseness parameter Δ_L by

$$|\tilde{\eta}(L_c)| = 1/2, \quad |\tilde{\eta}(L_c + 2.2\Delta_L)| = 0.9\,, \tag{6}$$

where $\tilde{\eta}(l)$ represents $\eta_a(l)$ or $\eta_B^{(0)}(l)$ in energy region III or II, respectively. In order to relate the quantities L_c and Δ_L to the optical potential parameters, we now remark that $r_1(l)$ or $r_a(l)$ for medium and high partial waves lie in the vicinity of the corresponding distance of closest approach for the Coulomb scattering $r_c(l)$. The JWKB formula for the phase shift then leads to [11],

$$2\delta_1(l) = 2\delta_a(l) = \frac{1}{\hbar v}\left\{\frac{2\pi r_c}{1 - n/(kr_c)}\right\}^{1/2} \times \{V_0 a_R^{1/2} e^{-(r_c - R_R)/a_R} + iW_0 a_w^{1/2} e^{-(r_c - R_w)/a_w}\}\,, \tag{7}$$

and hence

$$\lambda = l + 1/2 \approx k\{R_w + a_w[-4.366 - \ln(\ln(|\eta(\lambda)|^{-1})) - \ln(v/c) + \ln(W_0) + \tfrac{1}{2}\ln(a_w)]\}\,. \tag{8}$$

In eqs. (7) and (8), the quantities v, n and k are the initial speed of the relative motion, the Coulomb parameter, and the wave number, respectively. In obtaining eq. (7), we have assumed an optical potential with the Woods–Saxon form factor and have used the asymptotic form, because in the relevant energy region $r_c(l)$ lies in the tail region of the optical potential. For the cut-off angular momentum defined by eq. (6), the various terms in the square bracket in eq. (8) almost cancel against each other. We thus obtain

$$\lambda_c = L_c + 1/2 \approx k \cdot R_w\,. \tag{9}$$

From eqs. (6) and (8) it follows directly that

$$\Delta_L = 0.856\, k \cdot a_w\,. \tag{10}$$

Eq. (9) and a formula similar to eq. (10) have often been used in analyzing data of heavy-ion collisions. To the author's knowledge, however, the derivation of these equations [10] seems not to have been clear so far [12].

The prediction of eqs. (9) and (10) agrees very well with the numerical results of eqs. (2) and (4). This clearly shows that the imaginary potential plays the decisive role in determining the behaviour of $|\eta(l)|$ at medium and high energies. This contrasts with the case of low energy scattering from an optical potential with a deep real part [5]. In that case, λ_c is mostly determined by the real potential and is close to the grazing angular momentum λ_{gr}, for which the top of the effective potential barrier coincides with the incident energy and $|\eta_B(\lambda_{gr})| = 2^{-1/2}$. The diffuseness parameter Δ_L is strongly affected by the barrier penetrability and hence is essentially determined by the factor N. Accordingly, it is well represented in terms of the quantities specifying the surface properties of the effective real potential and not those of the imaginary potential [5].

In fig. 1, the classical deflection function $\Theta(\lambda = l + 1/2)$ has been calculated by taking the difference of the real part of the phase shift at $l + 1$ and l. We notice that $\Theta(\lambda)$ for $E_\alpha = 200$ MeV exhibits a nuclear rainbow at $-43°$. For 40 and 99.5 MeV, we have separately given the deflection functions corresponding to the barrier and the internal wave S matrices. Though one observes a nuclear rainbow in Θ_I, it does not play any role, because $|\eta_I|$ is very small at the rainbow angular mo-

mentum. One might try to combine $\Theta_B(l)$ and $\Theta_I(l)$ in order to obtain a deflection function corresponding to the total S matrix $\eta(l)$ which looks similar to $\Theta(l)$ in the energy region III and shows a nuclear rainbow. The result would, however, not be very reliable because at low and at medium energies the phase of $\eta(l)$ changes very drastically around the transitional angular momentum where the dominance of $\eta_B(l)$ replaces the dominance of $\eta_I(l)$.

Fig. 2 shows the cross sections as calculated by the partial wave summation of the scattering amplitudes. The semiclassical S matrices at 200 MeV and at 99.5 MeV are given by eqs. (2) and (3), respectively. At 200 MeV the semiclassical calculation agrees very well with the quantum calculation. The cross section at 99.5 MeV has been decomposed according to the splitting of the S matrix [4]. The agreement between the quantum and the semiclassical calculations at this energy is not so good as that at 200 MeV. Nevertheless, the general structure of the angular distribution in the quantum calculation is well reproduced by the semiclassical calculation. The remarkable thing is that the gross hump at medium angles for this energy is caused by the interference between the barrier and the internal waves and is not related to rainbow scattering. Concerning the hump observed in the angular distribution in energy region II, we are thus led to a quite different picture from that of refs. [2,3,7], where the authors attribute it to a nuclear rainbow effect. Notice that the similar interference effect is absent at 200 MeV. This indicates that the origin of the gross hump in energy region III is completely different from that in energy region II, although in both energy regions the imaginary potential plays an important role.

In conclusion, the semiclassical analysis of α–^{90}Zr scattering from an optical potential, which fairly well fits the experimental data, indicates that there exist two critical energies in the scattering of α particles from nuclei. In the low energy region (region I), there exist in general three active turning points for each partial wave. The interference between the barrier and the internal waves leads to a complicated oscillation pattern in the differential cross section over the whole angular range. At high energies (region III), there is only one important turning point for each partial wave. The gross hump observed at medium angles in the differential cross section might be associated with the nuclear rainbow which manifests itself in the classical deflection function. In the intermediate energy region (region II), the angular distribution looks very similar to that in region III. Nevertheless, there exist three important turning points for some surface partial waves due to the existence of the external potential barrier, though the role of the real potential is less important compared to the case of energy region I and the role of the imaginary potential becomes more decisive. The gross hump in the angular distribution is caused by the interference between the barrier and the internal waves and cannot be described as a rainbow phenomenon.

With the aim of directly determining the second critical energy from experimental data, we have studied the energy variation of Θ_M, the angle where the hump in $d\sigma(\theta)/d\sigma_R(\theta)$ is maximum, and of κ, the slope of $\ln(d\sigma(\theta)/d\sigma_R(\theta))$ beyond Θ_M, in the angular distributions for $\alpha + {}^{90}$Zr as calculated up to $E_\alpha = 300$ MeV for the potentials given by eq. (1). As the gross hump in the angular distribution arises from a different origin in energy regions II and III, one might expect significant changes in these quantities qround the second critical energy. We found, however, that neither $\theta_M(E_\alpha)$ nor $\kappa(E_\alpha)$ show evident changes around $\epsilon^{(2)}_{\alpha\mathrm{lt}}$. The curve $\kappa(E_\alpha)$ against $\sqrt{E_\alpha}$ shows a striking kink at $\bar{E} = 100$ MeV. The relation between $\bar{E}$ and the critical energies is, at this moment, not clear. Studies along this line are now in progress.

Most of this work has been done when one of the authors (N.T.) stayed at Universität Münster. He is grateful to Profs. R. Santo and A. Weiguny and to members of Theoretical Physics I and of Kernphysik of Universität Münster for their warm hospitality. He is pleased to acknowledge the financial support from the Bundesministerium für Forschung und Technologie.

References

[1] L.W. Put and A.M.J. Paans, Nucl. Phys. A291 (1977) 93.
[2] D.A. Goldberg, S.M. Smith and G.F. Burdzik, Phys. Rev. C10 (1974) 1362.
[3] D.A. Goldberg, Invited Talk presented at the Symp. on Heavy-ion elastic scattering (Rochester, NY, 1977).
[4] D.M. Brink and N. Takigawa, Nucl. Phys. A279 (1977) 159.
[5] N. Takigawa, Proc. Second Louvain–Krakow Seminar, eds. G. Grégoire and K. Grotowski (Louvain-la-Neuve, June 1978).
[6] I. Brissaud et al., Nucl. Phys. A191 (1972) 145.

[7] K.W. McVoy, Lectures presented at the Escuela Latino-Americana de Física (Universidad Nacional Autonoma de Mexico, 1977).
[8] S.Y. Lee, N. Takigawa and C. Marty, Nucl. Phys. A308 (1978) 161.
[9] K.M. Hartmann, preprint, Univ. of Oxford (1977).
[10] W.E. Frahn and R.H. Venter, Ann. Phys. (NY) 24 (1963) 243;
J.S. Blair, Lectures in theoretical physics, Vol. VIIIC, eds. P.D. Kunz et al. (Univ. of Colorado Press, 1966) p. 343.
[11] D.M. Brink, J. de Phys. C5 (1976) 47.
[12] See also D.M. Brink, Les Houches Lectures (1977), eds. R. Balian et al.